WORK IN PROGRESS “GEOTHERMAL CONCEPTUAL MODEL OF THE CUENCA ALTA DEL RÍO LAJA, GUANAJUATO, MEXICO”

Lucía Magali Ramírez-González, María Jesús Puy-Alquiza, Yanmei Li
University of Guanajuato

We support the Sustainable Development Goals

Introduction

The presence of hot springs in the Cuenca Alta del Río Laja (CARL) basin has been recognized by the local population since pre-Hispanic times. Since temperatures do not exceed 50°C, it is considered a low-temperature, low-enthalpy resource with the potential to be used as direct uses of geothermal energy.

The first part of this study used the temperature values of 101 wells distributed around the CARL from the INEGI database. The values were interpolated by using the geostatistical methods Inverse Distance Weighting (IDW) and Empirical Bayesian Kriging (EBK).

The second part of the research, which is carried out to date, consists of planning and taking water samples for geochemical analysis. First the samples were analyzed by using X-ray fluorescence (XRF) as a first scope, and then the main ions will be analyzed for the classification of water and the isotopes of $\delta^{18}O$ and δD to know the water origin.

Later stages of this work involve the construction of the conceptual model; the study of the relationship between high temperatures, arsenic and fluor concentrations, together with the correlation of temperatures with the recharge and discharge rates of the aquifer.

Methodology

We digitalized the geologic maps F14-7 and F14-10 from the Mexican GeoSurvey (SGM). Main fractures and faults were compiled from Alaniz-Álvarez *et al*., 2002.

Thermal manifestations were mapped from the inventory of González-Ruíz *et al*., 2015 and the list of thermal spas from the Balnearios de México website.

Hydrogeological information was taken from the hydrogeological map of the CARL from MGJJVNNVVYUI9999999999999999999999999IKIIIII88 INEGI, 2019.

We interpolated the measured water temperature of wells from the CARL basin compiled from INEGI (2019). The Inverse Distance Weighting method was carried out in R using a grid of 5000 x 5000 m pixel size (Figure 1). The geostatistical method Empirical Bayesian Kriging was carried out in ArcGIS 10.6.1 ® (Figure 2). The model used four interactions and the used parameters were: log empirical transformation, K-Besel semivariogram, smooth circular neighborhood type, smoothing factor of 0.3 and radius of 10000. 12 wells were identified as outliers and dismissed from the model.

The first stage of the geochemistry analysis so far was a set of four water samples marked as M-1 to M-4 in Figure 1 and Figure 2. The samples were taken on September 23rd, 2021. Physico-chemical analysis were taken *in situ*. We used a temperature probe for the temperature measurements, a pHep ® by Hanna for pH, a TDS&EC meter (hold), ammonia and CO_2 test by SSQuim, an iron test kit by Hanna, and paper test strips for the pH, alkalinity and chlorine.
The samples were also analyzed by using X-ray fluorescence (XRF) in the LICAMM lab from the University of Guanajuato. Results are shown in Table 1.

WLC18- 0032

Results

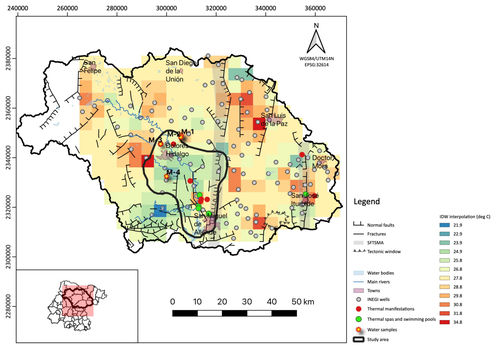

Figure. 1 Temperature interpolation map using the Inverse Distance Weighting.The main faults, the thermal manifestations, the sampled locations and the selected study area are shown as well.

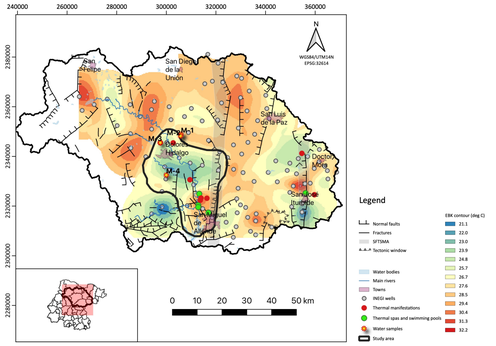

Figure. 2 Temperature prediction map from the Empirical Bayesian Kriging. The main faults, the thermal manifestations, the sampled locations and the selected study area are shown as well.

Table 1. *In situ* physico-chemical parameters from the water samples and chemical analysis from the XRF analysis.

	M-1	M-2	M-3	M-4
		in situ measurements		
Temp (deg C)	45.8	28.5	38.9	42.7
pH	8.2	8.4	8.2	8.5
EC (µs/cm)	675	556	354	426
TDS (ppm)	322	261	213	201
Cl (ppm)	<10	<10	<10	<10
Ammmoniac (mg/l)	0	0	0	0
Hardness	250	100	250	500
Cl (ppm)	3	3	4	3
Free Cl (ppm)	0.5	1	0	1
pH	8.4	8.4	7.8	8.4
Alcalinity (ppm)	240	240	240	180
Fe (mg/l)	<1	<1	<1	<1
CO_2 (ppm)	8	8	7.6	7.8
		FRX		
Mg (ppm)	2705	2660	5330	4379
K (ppm)	nd	193	nd	nd
Ca (ppm)	593	1010	487	615
Ti (ppm)	99.7	156.9	79.3	85
Y (ppm)	nd	nd	nd	nd
Zr (ppm)	137.4	182	145.5	43
Ru (ppm)	nd	983.815	nd	1199
Rh (ppm)	992892	991271	989760	989623
Ag (ppm)	133.8	nd	nd	nd
Al (ppm)	1499	1719	2064	2104
Si (ppm)	1179	1273	1216	1575
Ar (ppm)	68.3	nd	nd	nd
MgO (mass%)	nd	2.2845	1.8993	0.4917
K_2O (mass%)	0.935	1.039	0.0701	0.4829
CaO (mass%)	5.14	32.61	0.3331	27.6488
Al_2O_3 (mass%)	21.1	15.68	16.8	11.97
SiO_2 (mass%)	42.9	26.76	36.6	25.79
P_2O_5 (mass%)	2.12	1.0889	3.99	3.012
SO_3 (mass%)	24.1	11.845	35.1	23.16
TiO_2 (mass%)	1.565	1.129	0.1333	0.7738
MnO (mass%)	0.7291	1.068	3.848	1.897
Fe_2O_3 (mass%)	0.888	6.494	1.2695	4.774

Figure.3 Water from the Oasis well (M-3) at 38.9 deg C.

Conclusions

The geostatistical analysis shows that high temperature values align to major fault systems. The analysis of the temperature distribution together with geological and hydrogeological information and the inventory of thermal manifestations were used to delimit the study area which comprises a polygon of 855 km^2 between San Miguel de Allende and Dolores Hidalgo. It covers areas with contrasting values of temperature, it hosts the largest number of thermal manifestations and is located to the west of the Taxco-San Miguel de Allende Fault System (SFTSMA).
As, F, Cd, Pb, Cr, Na, K, Mg, Fe, S, Cl, SO_4 and HCO_3 were not detected by the XRF. Since those ions and elements are important for this study, samples will be further analyzed by ICP-MS and MP-AES.

Later stages of this work involve determining the continuity between the geothermal system of San Miguel de Allende and Dolores Hidalgo, its relationship with arsenic concentrations and the relationship of temperatures with the recharge and discharge rates of the aquifer.

Acknowledgments

I gratefully thank the DAIP and the Rectory Campus Guanajuato of the University of Guanajuato for the economical support for this project.

References

Alaniz-Álvarez, S.A., Nieto-Samaniego, A.F., Orozco-Esquivel, M.T., Vassallo, L.F., Xu, S., 2002. El sistema de fallas Taxco-San Miguel de Allende: Implicaciones de la deformación post-eocénica del centro de México. Boletín de la Sociedad Geológica Mexicana, Tomo LV, Núm., 1, 2002. P. 12-29

CONCYTEG-CFE, 2002. Evaluación preliminar de los recursos energéticos renovables en el estado de Guanajuato.

Balnearios de México. Retrieved on abri 2021 from: https://www.balneariosmexico.com

González-Ruiz, L.E., González E., Garduño-Monrroy, V.H., Martinez, L., Pironon, J., Díaz Carreño, E.H., Yáñez-Dávila, D., Romero-Rojas, W., Romero-Rojas, M.C., 2015. Distribución de Anomalías Geotérmicas en México: Una guía en la prospección geotérmica. RIIT, ISSn: 2007-9753.

INEGI, 2019. Zona Hidrogeológica Alta Río Laja Serie II, Escala 1:250,000. Conjunto de datos. Recuperado en febrero del 2021 de: https://www.inegi.org.mx/app/biblioteca/ficha.html?upc=889463769200

Kresic, N., Mikszewski, A., 2012. Hydrogeological Conceptual Site Models: Data Analysis and Visualization 600, pp.

Knappett, P., Li, Y., Loza., I., Hernandez, H., Avilés, M., Haaf, D., Majumder, S., Huang, Y., Lynch, B., Piña, V., Wang, J., Winkel, L., Mahlknecht, J., Datta, S., Thurston, W., Terrell, D., Nordstrom, D., 2020. Rising arsenic concentrations from dewatering a geothermally influenced aquifer in central Mexico. Water Research 185 (2020) 116257.

Nicholson, K., 1993. Geothermal fluids. Chemistry and Exploration Techniques. Springer-Verlag.

SGM (Servicio Geológico Mexicano), 1997. Carta geológica-minera Guanajuato F14-7.
SGM (Servicio Geológico Mexicano), 1999. Carta geológica-minera Querétaro F14-10.